Proceedings of the ASME 2019
Pressure Vessels & Piping Conference
PVP2019
July 14-19, 2019, San Antonio, TX, USA

PVP2019-93720

PROBABILISTIC RISK ASSESSMENT OF AGING LAYERED PRESSURE VESSELS

D. S. Riha[1,a], M. L. Kirby[1], J. W. Cardinal[1], L. C. Domyancic[1], J. M. McFarland[1], and F. W. Brust[2]
[1]Southwest Research Institute, San Antonio, TX
[2]Engineering Mechanics Corporation of Columbus, Columbus, OH

ABSTRACT

The National Aeronautics and Space Administration (NASA) operates approximately 300 aging layered pressure vessels that were designed and manufactured prior to ASME Boiler and Pressure Vessel (B&PV) code requirements. In order to make decisions regarding the continued fitness-for-service of these non-code carbon steel vessels, it is necessary to perform a relative risk of failure assessment for each vessel. However, risk assessment of these vessels is confounded by uncertainties and variabilities related to the use of proprietary materials in fabrication, missing construction records, geometric discontinuities, weld residual stresses, and complex service stress gradients in and around the welds. Therefore, a probabilistic framework that can capture these uncertainties and variabilities has been developed to assess the fracture risk of flaws in regions of interest, such as longitudinal and circumferential welds, using the NESSUS® probabilistic modeling software and NASGRO® fracture mechanics software. In this study, the probabilistic framework was used to predict variability in the stress intensity factor associated with different reference flaws located in the head-to-shell circumferential welds of a 4-layer and 14-layer pressure vessel. The probabilistic studies predict variability in flaw behavior and the important uncertain parameters for each reference flaw location.

Keywords: Layered Pressure Vessel, Head-to-Shell Circumferential Weld, Fitness for Service, Risk Assessment, Verification and Validation, Probabilistic Methods, Stress Intensity Factor, Finite Element Analysis

INTRODUCTION

In order to support a larger effort by the National Aeronautics and Space Administration (NASA) to assess the fitness for service of aging layered pressure vessels (LPVs), which was initiated under a previous NASA Engineering and Safety Center effort [1], this research sought to develop a probabilistic framework for predicting the relative risk of fracture of existing vessels in NASA's fleet. A considerable range of materials, stress states, and geometry and number of layers (from 3 to 32-layer LPVs) are represented in this fleet of nearly 300 vessels. In addition to variations among the vessels, their construction and operating conditions, there is uncertainty in the geometry (e.g. layer thickness, interlayer gaps/vessel efficiency, weld width, etc.), weld residual stress, and material properties (e.g. fracture toughness) for a given vessel in the fleet. Traditional fitness for service approaches may be overly conservative due to the many unknowns in these vessels. Therefore, a probabilistic framework, with enough flexibility to model every vessel in the diverse fleet of LPVs, was needed to quantify these uncertainties and understand their effect on fitness for service of a given vessel.

To demonstrate the probabilistic framework developed in this research, two reference flaws in a 4- and 14-layer head-to-shell (H-S) circumferential weld were evaluated, and global sensitivities and cumulative distributions of the stress intensity factor (SIF) were calculated for the reference flaws. The H-S welds of these vessels have a unique geometry and stress state, with interlayer gaps coming into the weld and introducing bending stress and complex weld residual stress fields from fabrication. Additionally, LPV H-S welds are challenging to inspect with current industry-standard non-destructive evaluation (NDE) techniques warranting the development of models to predict important flaw sizes, orientations, and locations within the weld to guide NDE requirements and potential development efforts. Ultimately, the probabilistic results of this study provide insight into how material, geometry, and weld residual stress uncertainties influence the model predictions for larger (14-layer) and smaller (4-layer) vessels within the fleet and opportunities to improve models and/or gather additional experimental data to reduce uncertainty in the predictions.

[a] Contact author: david.riha@swri.org

MATERIALS AND METHODS

Verification, Validation, and Uncertainty Quantification

Model development using a verification and validation (V&V) framework provides a systematic approach to identify important phenomena, quantify uncertainties and approximations, and establish evidence about the predictive accuracy of the models. Guidelines are available for such areas as solid mechanics models [2] and integrated computational materials engineering models [3] to name a few. Uncertainty quantification plays an important role in V&V by quantifying the impact of errors, uncertainties, and variations on prediction variability. Variations can be any naturally occurring variability in materials and loadings. Errors may be approximations in the models such as choice of constitutive models or mesh discretization. Uncertainties are defined as lack of knowledge such as limited experimental data to define model inputs or not knowing the precise geometric configuration of a structure. These can all be termed uncertainties and defined by probability density functions (PDF). Probabilistic methods can then be used to propagate the uncertainties through the models to predict the variability in the response. Probabilistic sensitivity methods can also be used to identify how much each uncertainty contributes to the prediction. These sensitivities provide a systematic way to make decisions about ignoring, reducing, or incorporating each uncertainty in the models. These sensitivities also support decisions about resource allocation for model improvements and experiments to improve accuracy and reduce uncertainty.

Probabilistic Methods

Mature probabilistic and uncertainty quantification (UQ) methods and tools exist to quantify uncertainties in the model predictions due to uncertain inputs, such as Monte Carlo simulation, Bayesian analysis, and fast probability integration methods. These methods can be used to predict the probabilistic response in the form of a cumulative distribution function (CDF) or PDF. The reliability or probability of failure can be computed by formulating a limit-state to define a failure condition such as the stress intensity factor exceeding the fracture toughness. The limit-state function, g, separates the safe and failed regions in the design space. It is usually formulated such that negative values indicate combinations of variables leading to failure:

$$g = K_{JC} - K_I = 0 \qquad (1)$$

where K_I is the stress intensity and K_{JC} is the elastic-plastic fracture toughness. Then the probability of failure is defined by:

$$p_f = P[g < 0] = P\left[K_{JC} - K_I < 0\right] = P\left[K_{JC} < K_I\right] \qquad (2)$$

The probability in the failure region is determined by integrating the joint PDF (f_X) of all random variables (X) over the region:

$$p_f = \int_{g<0} \dots \int f_X(x)dx \qquad (3)$$

Appropriate probabilistic methods are selected to perform this integration depending on the computational effort to evaluate the limit-state function and the required accuracy.

Both global and local probabilistic sensitivity factors can be computed. One local sensitivity is the derivative of the probability of failure with respect to input random variable distributions. These sensitivities identify the input variations contributing the most to the probability of failure. A global sensitivity is based on variance decomposition [4]. These sensitivities identify the contribution of each parameter to the overall predicted variance or probabilistic response as compared to a single probability value. The global sensitivities include main effects (how much each variable contributes independently) and total effects (how each variable along with its interactions with other variables contributes).

Many of these methods are available in the NESSUS® probabilistic analysis software [5]. NESSUS was originally created by a team led by Southwest Research Institute as part of a 10-year NASA project started in 1984 to develop a probabilistic design tool for the space shuttle main engine with a focus on probabilistic finite element analysis. NESSUS has seen constant development ever since, leading to a full graphical user interface, additional methods, and interfaces to many third-party codes such as Abaqus, ANSYS, LS-DYNA, MSC.NASTRAN, and NASGRO®.

Vessel Materials and Geometry

A 4-layer (1 inner layer and 3 wrapped shell layers) and 14-layer (1 inner layer and 13 wrapped shell layers) vessel were selected from NASA's LPV fleet as demonstration vessels. These vessels were manufactured by the Chicago Bridge and Iron Company in 1963, and information about the geometry and materials used to construct these vessels was obtained from the construction records. The inner layer of the vessels was rolled from 1143 Mod. steel, the shell layers were rolled from 1146 steel, and the vessel head was fabricated from A-225 Grade B firebox quality steel. Rolled segments of the inner layer were joined together via a longitudinal seam weld, and shell layers were tightly wrapped around the inner layer and welded in the same manner to form shell courses. The courses were welded together with multi-pass shell-to-shell (S-S) circumferential welds to form the cylindrical body of the vessel. Similarly, the hemispherical head was joined to the cylindrical vessel by a multi-pass head-to-shell (H-S) circumferential weld. The modulus of the inner layer, shell layer, head, and weld material was assumed to be 2.95×10^7 psi for linear elastic stress analysis.

Uncertainty in the inner layer thickness, shell layer thickness, head thickness, and the width of the H-S weld were estimated based on the vessel construction records and expert opinion from the pressure vessel manufacturing community. In addition, uncertainty in vessel efficiency due to interlayer gaps was quantified using pi tape measurements of the diametric expansion of LPVs at NASA's Ames Research Center. A total of 139 individual shell course pi tape measurements were recorded and a beta distribution was fit to the vessel efficiency data using maximum likelihood estimation. One advantage afforded by the

TABLE 1: 4-LAYER VESSEL GEOMETRY AND LOADING/BOUNDARY CONDITION (BC) INFORMATION

	Design	Distribution	Parameters
Geometry			
Head Thickness	1.056[c] in	uniform[d]	a=1.056 b=1.1088
Diameter	24 in	deterministic	
Length[a]	118 in	deterministic	
Inner Layer Thickness	0.50[c] in	uniform	a=0.50 b=0.54
Shell Layer Thickness	0.25[c] in	uniform	a=0.25 b=0.29
Efficiency	≥ 50%	beta	α=7.8207 β=3.0674 L=50 U=100
H-S Weld Width	0.875 in	uniform[e]	a=0.7437 b=1.0063
Loads/BCs			
Pressure[b]	3500 psi	deterministic	
Coefficient of Friction	0.7	deterministic	

[a]tangent-to-tangent vessel length
[b]maximum allowable working pressure (MAWP)
[c]minimum
[d]variable range: -0, +5% from design
[e]variable range: ±15% from design

TABLE 2: 14-LAYER VESSEL GEOMETRY AND LOADING/BOUNDARY CONDITION (BC) INFORMATION

	Design	Distribution	Parameters
Geometry			
Head Thickness	3.699[c] in	uniform[d]	a=3.699 b=3.8840
Diameter	60.25 in	deterministic	
Length[a]	720 in	deterministic	
Inner Layer Thickness	0.46875[c] in	uniform	a=0.46875 b=0.50875
Shell Layer Thickness	0.28125[c] in	uniform	a=0.28125 b=0.32125
Efficiency	≥ 50%	beta	α=7.8207 β=3.0674 L=50 U=100
H-S Weld Width	1.0625 in	uniform[e]	a=0.9031 b=1.2219
Loads/BCs			
Pressure[b]	5000 psi	deterministic	
Coefficient of Friction	0.7	deterministic	

[a]tangent-to-tangent vessel length
[b]maximum allowable working pressure (MAWP)
[c]minimum
[d]variable range: -0, +5% from design
[e]variable range: ±15% from design

use of a beta distribution to describe the vessel efficiency is that beta distributions have an upper and lower bound. A vessel efficiency above 100% is a physical impossibility and the ASME code [6] requires vessels to have an efficiency greater than 50% to be used in service. Table 1 and Table 2 show the vessel geometry, along with the maximum allowable working pressure and an estimated coefficient of friction governing the sliding behavior of layers that are in contact with one another, for the 4- and 14-layer vessel respectively,. Previous sensitivity studies have shown that variation and uncertainty in the coefficient of friction do not influence the stress field in the circumferential welds, but it has a significant impact on the stress field in the longitudinal seam welds [7]. Therefore, the coefficient of friction was treated as a deterministic variable in this study.

Fracture toughness for the different materials at different conditions for the fleet of vessels is being determined experimentally. Some of these ferritic steels can potentially experience cleavage cracking at operating temperatures depending on the geographic location of the vessel. Therefore testing using the ASTM E-1921 standard is being used to determine the reference temperature, T_o, in the transition range. Once T_o has been determined, the standard includes an equation to calculate the fracture toughness over a range of temperatures along with a Weibull distribution of the variation. Because there is uncertainty on when the cleavage behavior transitions to the upper shelf, a probabilistic model was developed to use the lower value of either the cleavage or upper shelf fracture toughness. These models are shown in Figure 1 with 5% and 95% tolerance bounds and random samples for a range of temperatures.

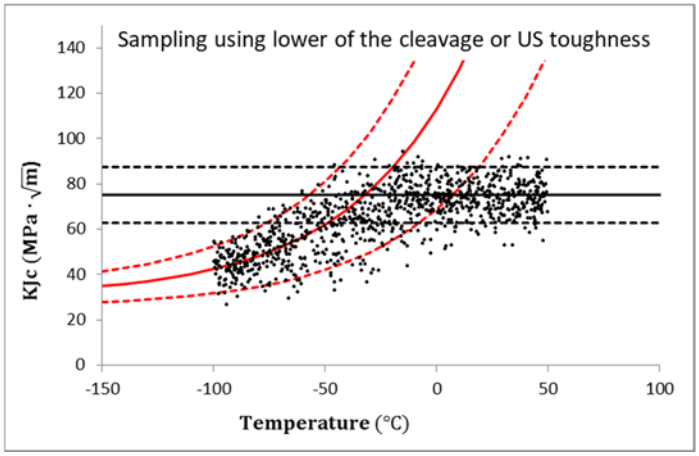

FIGURE 1: CLEAVAGE FRACTURE TOUGHNESS MODEL USING ASTM E-1921 SHOWN IN RED. UPPER SHELF FRACTURE TOUGHNESS SHOWN IN BLACK. 5% AND 95% TOLERANCE BOUNDS ARE REPRESENTED BY DOTTED LINES. BLACK CIRCLES ARE RANDOM SAMPLES USING THE COMBINED MODELS.

In order to demonstrate the probabilistic framework, two semi-elliptical reference flaws in the H-S weld were analyzed as shown in Figure 2. One of the reference flaws was a transverse (axially oriented) crack in the heat-affected zone of the H-S weld, on the head-side of the weld, growing radially from the inner

surface of vessel. The other flaw was a circumferential crack near the fusion line of the H-S weld, on the shell-side of the weld, also growing radially from the inner surface of the vessel. These locations were selected for the reference flaws because they are locations where flaws have been observed and/or they are locations that are challenging to inspect with current NDE capabilities. Observed flaws were believed to be manufacturing flaws because there has been no indication of crack growth in these locations. In addition, two flaw geometries were evaluated for each flaw location. The first flaw geometry was equivalent to an ASME code reference flaw with a crack depth (a) of 0.25 in and an aspect ratio (a/c) of 1, and the second was a shallow flaw with a crack depth of 0.2 in and an aspect ratio of 2/3. Note that "a" is crack depth and "c" is half the surface crack length.

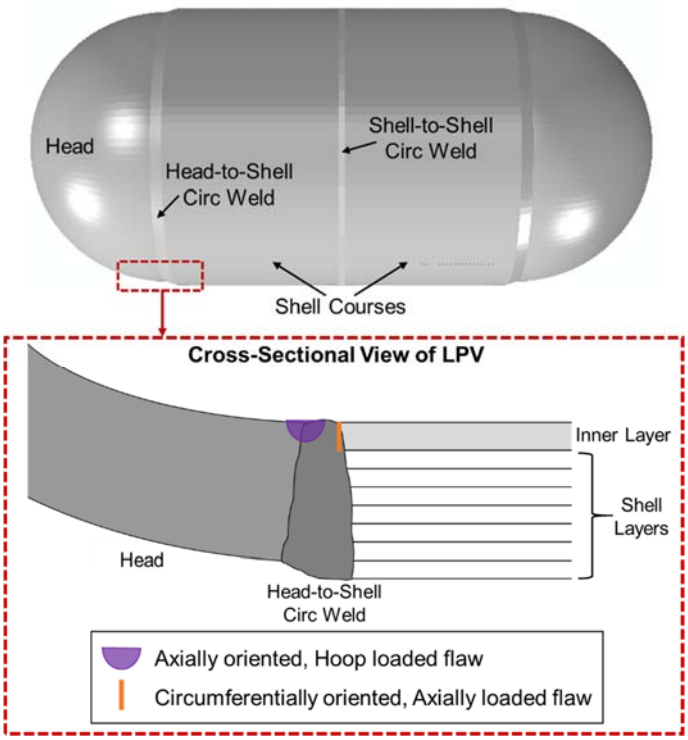

FIGURE 2: THE REGION OF INTEREST WITHIN THE VESSEL, FOCUSING ON THE HEAD-SHELL CIRCUMFERENTIAL WELD AND TWO REFERENCE FLAWS WITHIN THE WELD.

Probabilistic Framework and Supporting Models

The probabilistic framework developed in this research is a connection of analytical and numerical models that are exercised by NESSUS, in such a way that the output of one model is used as an input to the subsequent model. Input parameters can be defined as random variables according to a probability density function, and NESSUS randomly samples the input parameter distributions to perform global sensitivity analysis and full CDF analysis probabilistic studies. The probabilistic fracture risk of flaws in both the longitudinal seam and circumferential welds have been evaluated using this framework. However, this study was concerned with the treatment of flaws in the H-S circumferential weld, and thus, only the supporting models that are related to this end are discussed. The flow of the probabilistic analysis framework for a circumferential weld is shown in Figure 3 and can be summarized in four steps:

1. Vessel efficiency and basic vessel geometry are used to determine the sizes of interlayer gaps based on an assumed distribution of the gaps through the thickness.
2. The interlayer gaps are incorporated into a finite element model of the vessel to simulate the service stress gradient.
3. The service stress gradient is superimposed with the weld residual stress (WRS) gradient extracted from a separate finite element weld simulation to obtain the crack driving force for fracture analysis.
4. The superimposed stress is used in NASGRO to predict the SIF, failure assessment diagram, and/or critical crack size for fracture risk assessment.

Only the SIF predictions are shown in this study, however, the probabilistic framework also supports failure assessment diagram (FAD) and critical crack size (CCS) fracture risk assessment. The four supporting models used to predict the SIF in the H-S weld are (1) an analytical Excel-based "Gap Closure Tool" that predicts gap sizes and closure pressures, (2) a parametric axisymmetric finite element model that predicts the axial and hoop service stress gradients in the H-S weld, (3) a thermo-mechanical finite element weld simulation that predicts the residual stress field in the H-S weld, and (4) a NASGRO fracture mechanics model that calculates the SIF for a semi-elliptical crack in a flat plate.

Gap Closure Tool

The Gap Closure Tool is an Excel-based tool that was developed at NASA's Marshall Space Flight Center for predicting the size (thickness) of interlayer gaps through the thickness of the vessel and the resulting closure pressure due to the gaps. As the vessel is pressurized, the interlayer gaps close in succession from the inner to outer diameter of the vessel, and the applied pressure is not fully transferred to the outermost layer because some of the pressure (energy) is used to close the gaps. The pressure that is transferred to the outermost layer of the vessel during pressurization is referred to as the closure pressure, and the ratio of closure pressure to applied pressure is equivalent to the vessel efficiency. Basic vessel geometry (i.e., internal diameter, inner layer thickness, shell layer thickness, and number of layers), material properties (i.e., Young's Modulus and Poisson's ratio, which is 0.3 since these are steel vessels), the vessel efficiency, the maximum allowable working pressure, and an assumed distribution of the interlayer gaps through the thickness of the vessel are provided as inputs to the Gap Closure Tool model. Then, using thin-walled vessel theory and the associated analytical equations, the Gap Closure Tool uses Excel's Goal Seek function to change the size of the interlayer gaps until the ratio of the predicted closure pressure to the maximum allowable

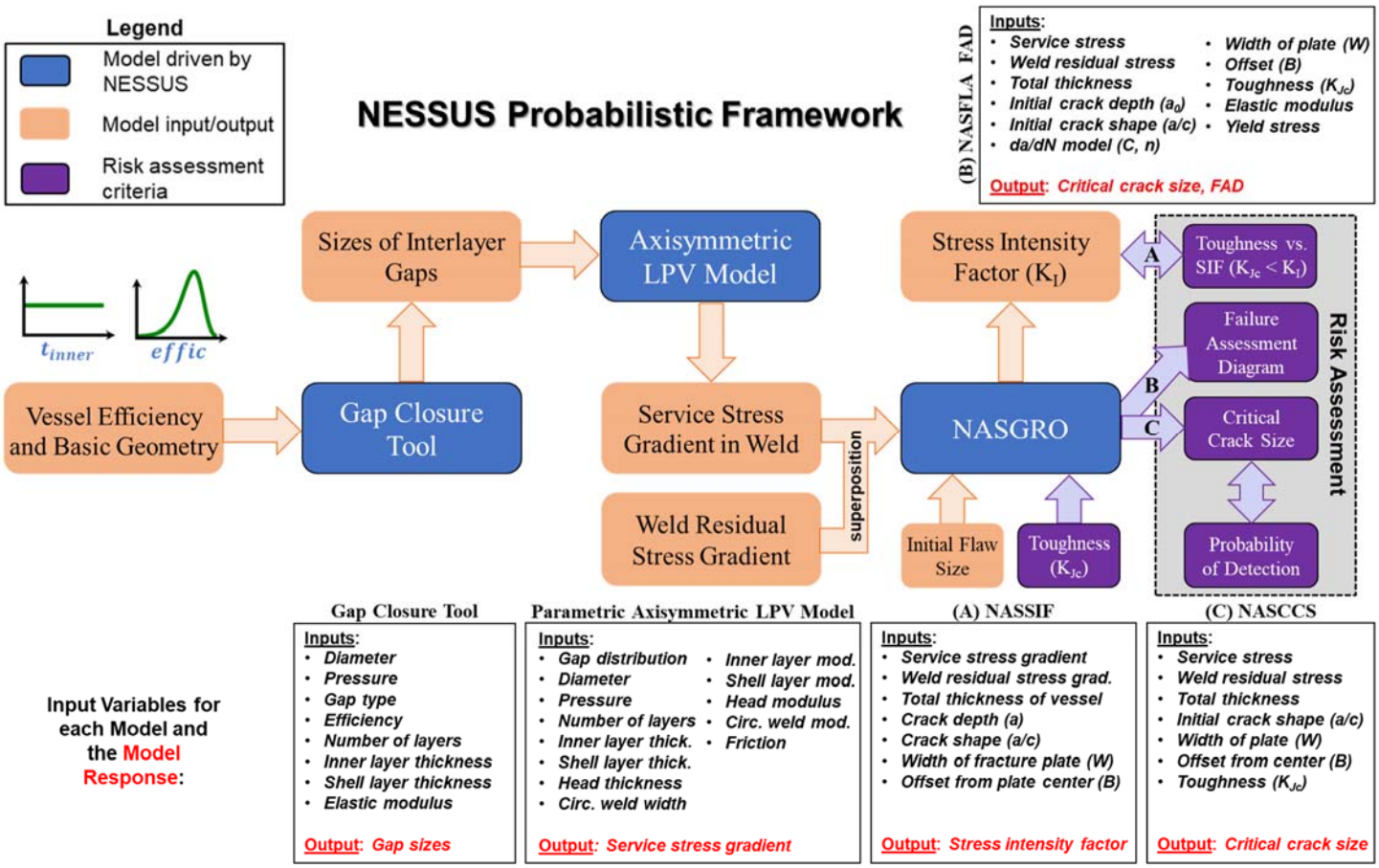

FIGURE 3: FLOWCHART OF THE PROBABILISTIC FRAMEWORK FOR PREDICTING FRACTURE RISK OF A FLAW IN A CIRCUMFERENTIAL (CIRC.) WELD.

working pressure is equal to the prescribed vessel efficiency. The resulting far-field radial, hoop, and axial stress are also calculated for each layer in the vessel. For this study, the distribution of the interlayer gaps through the thickness was assumed to be uniform, meaning that each interlayer gap had the same size through the thickness of the vessel. In general, the real distribution is thought to be linearly increasing through the thickness, meaning that the smallest interlayer gap is between the inner layer and the first shell layer and the largest gap is between the outermost shell layers. Therefore, the uniform gap distribution assumption was understood to be conservative because larger than expected gaps were prescribed between the innermost layers of the vessel, which increased the stress in the innermost layers.

Parametric Axisymmetric LPV Model

The parametric axisymmetric LPV model is a linear elastic finite element model of the vessel (Figure 4). Vessel geometry, material properties, the service stress (maximum allowable working pressure), and the gap sizes calculated by the Gap Closure Tool are provided as inputs to the model, and the model predicts the linear elastic stress field in the vessel during service. The model takes advantage of the axisymmetric nature of the vessel and the circumferential welds to reduce the order of the simulation from three-dimensions to two-dimensions, which reduces the computational cost of the simulation without significantly effecting the fidelity of the results. Additionally, a symmetry boundary condition is prescribed through the center of the S-S circumferential weld a distance of $2 \times (1.78\sqrt{rt})$ away from the H-S weld, where r is the internal radius of the vessel and t is the thickness of the vessel, or one diameter away from the H-S weld, whichever is the larger of the two, to further reduce the computational cost of the simulation. The significance of $1.78\sqrt{rt}$ is that applied forces and moments at one end of the vessel reduce to approximately 1% of their original value and have a negligible effect on the stress field at this distance [6,8]. Multiplying by two accounts for stress concentrations in both the H-S and S-S weld. In other words, the stress field in the H-S and S-S weld have a negligible effect on the far-field stress a distance of $1.78\sqrt{rt}$ from each weld.

The parametric axisymmetric LPV model was programmed as a Python script to be run within Abaqus Unified FEA, by Dassault Systèmes®, and the model is capable of simulating all of the LPVs in NASA's fleet. Some notable limitations of the model are that it does not consider the effects of longitudinal welds (increase stiffness due to the connection to the layer below the longitudinal weld) on the predicted stress field, it is not

capable of simulating a gap size of zero (the minimum interlayer gap thickness is 2E-6 in), it does not include the through-thickness weld taper of the circumferential welds, and it does not include the weld backing plate in the modeled geometry.

A Python script was also developed to extract the univariate hoop and axial stress gradients along a specified path after the finite element simulation in Abaqus. The starting and ending coordinates of the extraction path are provided as inputs to the script. Then the script calls an Abaqus routine for averaging the interpolated stress at the nodes in the proximity of one hundred equally spaced points along the path. This averaging routine allows the path to be mesh independent and results in a smooth stress gradient. The stress extraction paths used to obtain the service stress gradients are shown in Figure 4.

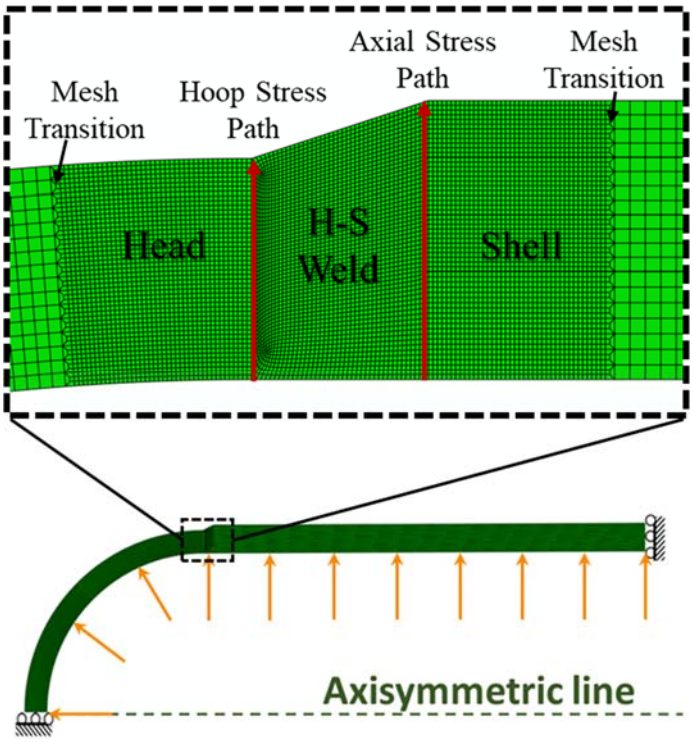

FIGURE 4: EXAMPLE OF THE PARAMETRIC AXISYMMETRIC LPV MODEL, FOCUSING ON THE MESH IN THE VICINITY OF THE H-S WELD AND THE STRESS EXTRACTION PATHS THROUGH THE THICKNESS OF THE VESSEL.

A mesh convergence study indicated that sufficient convergence occurred at an element density of roughly 45 elements/in^2. However, a mesh with this refinement is only necessary in the region of interest (the H-S weld). Therefore, a mesh transition, which performed a three to one mesh reduction from the H-S weld region to the far-field stress region, was used to further reduce computational cost. It was shown that this mesh transition could be located as close as a distance of one weld width away from the H-S weld boundary without significantly influencing the stress field in the H-S weld.

Thermo-mechanical Weld Simulation Model

Multi-pass weld simulations of the 4- and 14-layer H-S weld were performed by the Engineering Mechanics Corporation of Columbus (EMC^2) using the VFT^{TM} (Virtual Fabrication Technology) code [9], which utilizes a sequentially coupled thermal mechanical finite element analysis to predict the residual stress field in the weld [10]. These weld simulations included a hydro test mechanical simulation, in which the vessels were pressurized to 1.5 times the maximum allowable working pressure. All of the WRS gradients used in the study were extracted after the hydro test simulation. The nominal finite element stress contour plots for the 4- and 14-layer vessel after hydro test are show in Figure 5. The univariate WRS gradients were extracted from the weld simulations using a similar Python script to the one used to extract the service stress gradients from the parametric axisymmetric LPV model.

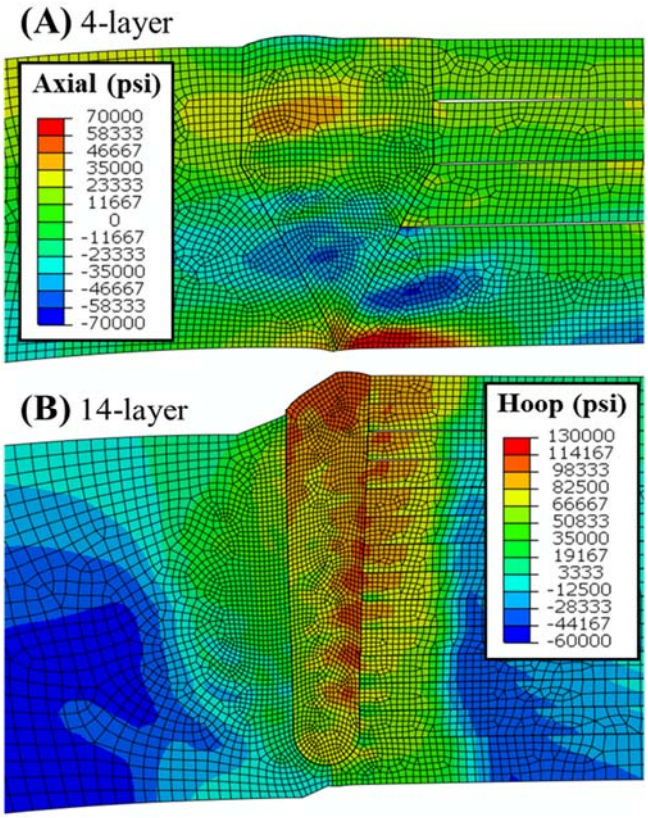

FIGURE 5: NOMINAL H-S WELD RESIDUAL STRESS CONTOUR PLOTS AFTER HYDRO SHOWING (A) AXIAL STRESS IN THE 4-LAYER VESSEL AND (B) HOOP STRESS IN THE 14-LAYER VESSEL.

Temperature dependent stress strain curves were determined experimentally for the different materials in the vessels. Variations of the material properties in the WRS Abaqus models were included by treating the temperature dependent coefficient of thermal expansion (CTE) and the stress-strain curves as random variables. Variations in these properties were assumed to follow a normal distribution with a 5% coefficient of variation (COV), based on expert opinion from the metallics and

reliability communities. Figure 6 shows the stress-strain curves for the A-225 Grade B steel with plus and minus three standard deviation bounds. Each random variable was mapped to the tabular Abaqus input to modify these inputs based on the changes in the random variables. The NESSUS software has capabilities to define this mapping once, and then create the Abaqus input file for any value of the random variable. There were six random variables: yield strength and CTE for each of the three materials (head, weld, and shells). Monte Carlo sampling was used to create training data in the form of hoop and axial stress gradients to develop the probabilistic WRS model. These 25 samples generated the gradients shown in Figure 7. Including variations in the material properties results in a large variation in the hoop stress gradients.

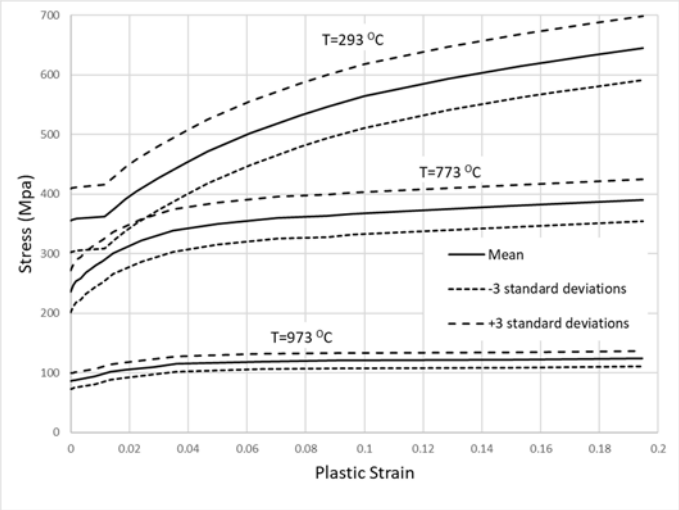

FIGURE 6: TEMPERATURE DEPENDENT STRESS-STRAIN CURVES FOR A-225 GRADE B STEEL WITH PLUS AND MINUS THREE STANDARD DEVIATION BOUNDS.

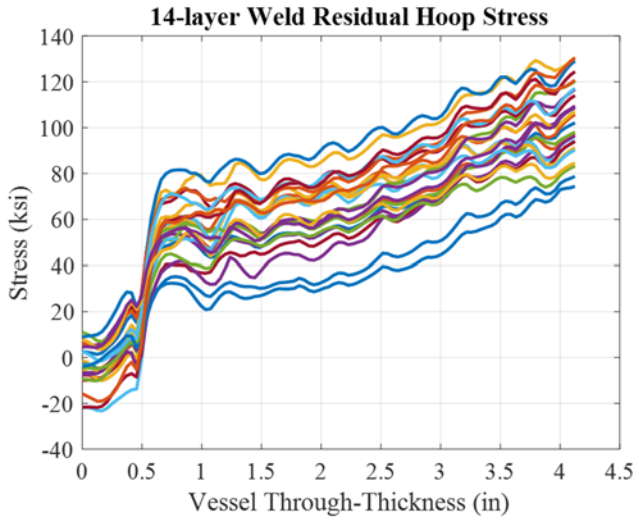

FIGURE 7: H-S WELD RESIDUAL HOOP STRESS GRADIENTS OF A 14-LAYER VESSEL AFTER HYDRO FOR 25 RANDOM SAMPLES OF THE MATERIAL PROPERTIES.

NASGRO Fracture Mechanics Model

A NASGRO [11] linear elastic fracture mechanics model of a semi-elliptical surface crack in a flat plate (SC30, which is a weight function solution) was used to predict the SIF (Figure 8). The univariate service stress and univariate WRS gradients were superimposed to create the stress field for which the SIF was computed. NASGRO also contains a fracture mechanics model that supports a bivariate stress field (SC31); however, an earlier study indicated that there was not a significant difference between the SIF results when using a univariate or bivariate stress gradient. In this study, the width of the plate (W) was half the circumference of the vessel, the thickness of the plate was equal to the thickness of the vessel, and the reference flaws were centered in the plate ($B = \frac{W}{2}$).

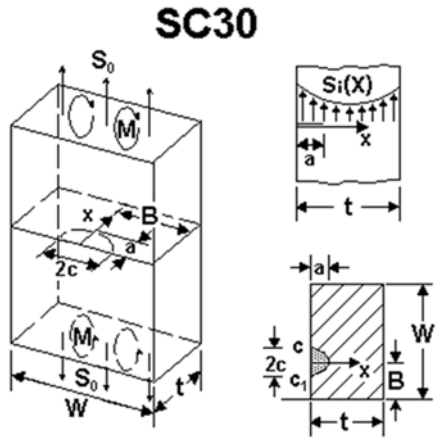

FIGURE 8: NASGRO FRACTURE MODEL SC30 USED TO COMPUTE THE SIF FOR A SEMI-ELLIPTICAL CRACK IN A FLAT PLATE.

Surrogate Modeling Approach

An innovative principal component analysis technique was used to create a surrogate model for the service stress and WRS gradients. The use of surrogate models to predict the service stress and WRS gradients in the probabilistic framework, instead of finite element models, greatly reduced the computational time necessary to perform the probabilistic analysis. It was not practical to include the parametric axisymmetric LPV model and thermo-mechanical weld simulation finite element model directly within the probabilistic framework, due to the computational cost. In order to accelerate the stress gradient calculations, a surrogate modeling approach was used. The purpose of the surrogate model was to rapidly predict the stress gradient as a function of selected input variables (such as head thickness, gap efficiency, etc.).

Response surface modeling approaches such as Gaussian Process regression [12] can be used to develop surrogate models based on a limited set of "training data" obtained through evaluation of the full model at a selected set of input conditions. One of the key challenges with development of a surrogate for the stress gradient is that the surrogate is required to predict the

stress at multiple points, as opposed to at a single location. In other words, the surrogate model output is a vector quantity. In order to address this, principal components analysis (PCA) was used to reduce the dimensionality of the model output [13].

The approach for developing each surrogate model involved three steps. First, a design of computer experiments was executed to generate training data in which the finite element analysis was repeated for a selected set of input conditions, producing a set of stress gradients. Second, PCA was used to express the variation in the stress gradient results as a linear combination of shape vectors (a.k.a. mode shapes). By retaining only the most important shape vectors, the dimensionality of the stress gradient can be significantly reduced. The singular values obtained from the PCA indicate the amount of variation explained by each shape vector. A given stress gradient can then be expressed in terms of a low-dimensional set of principal component scores (a.k.a. weights). The final step was to create individual response surface models to predict each principal component score as a function of the input variables. Here, Gaussian process regression was used. The surrogate model was applied by first predicting the principal component scores from the input variables and then reconstructing the stress gradient as a linear combination of the retained shape vectors. The predicted stress gradients were then used in NASGRO to compute the SIF.

RESULTS AND DISCUSSION

The nominal service stress and weld residual stress (WRS) gradients in the H-S weld for the two reference flaw locations are shown for the 4- and 14-layer vessel in Figure 9 and Figure 10 respectively. In addition, the nominal hoop stress contour plot at the maximum allowable working pressure is shown for the 4-layer vessel in Figure 11A, and the nominal axial stress contour plot at the maximum allowable working pressure is shown for the 14-layer vessel in Figure 11B. The service stress contour plots were visually obscured by the high mesh density in the H-S region, and thus, the mesh is not shown in the contour plots.

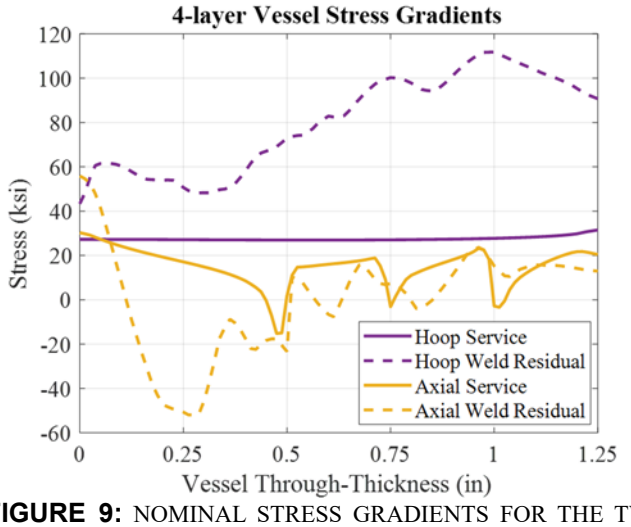

FIGURE 9: NOMINAL STRESS GRADIENTS FOR THE TWO REFERENCE FLAW LOCATIONS IN THE 4-LAYER VESSEL.

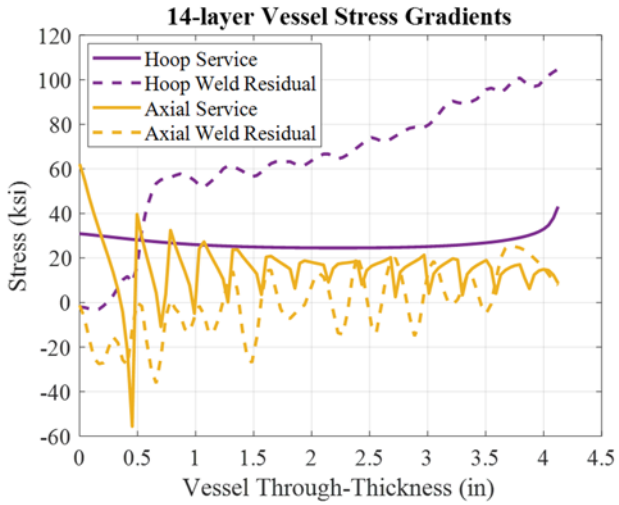

FIGURE 10: NOMINAL STRESS GRADIENTS FOR THE TWO REFERENCE FLAW LOCATIONS IN THE 14-LAYER VESSEL.

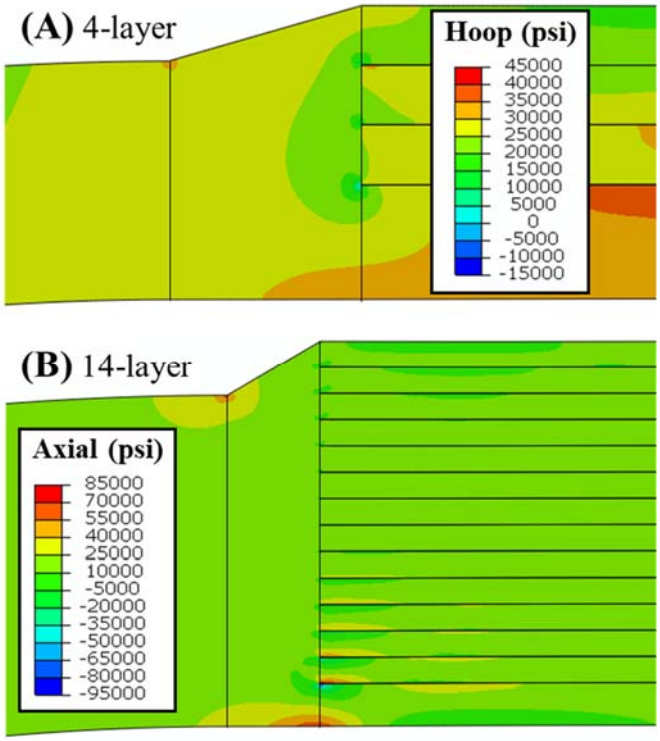

FIGURE 11: NOMINAL H-S SERVICE STRESS CONTOUR PLOTS FROM THE PARAMETRIC AXISYMMETIC LPV MODEL SHOWING (A) HOOP STRESS IN THE 4-LAYER VESSEL AND (B) AXIAL STRESS IN THE 14-LAYER VESSEL.

NESSUS was used to determine the sensitivity of the SIF to the random variables in the framework, which were vessel geometric parameters (see Table 1 and Table 2) and material properties (coefficient of thermal expansion and stress-strain curves) used in the weld simulations. The sensitivities to the materials used in the weld simulations were grouped into a single

weld residual stress variable, and the results of the global sensitivity analysis are shown in Figure 12 and Figure 13. The flaw geometry did not have a significant effect on the results of the sensitivity analysis, and thus, only one sensitivity plot is shown for each flaw location. Variability in the axially oriented, hoop loaded flaw SIF was dominated by variation in the weld residual stress, and the sensitivity results were nearly identical for the 4- and 14-layer vessels. Variation in the weld residual stress was also the primary sensitivity for the circumferentially oriented, axially loaded flaw in the 4-layer vessel (0.62), however, variation in the vessel efficiency (0.38) contributed to variability in the SIF. In contrast, the sensitivity results for the circumferentially oriented, axially loaded flaw in the 14-layer vessel showed that SIF variability is primarily sensitive to vessel efficiency variation (0.63) and secondarily sensitive to variation in the weld residual stress (0.24). It makes sense that vessel efficiency variation has more of a contribution to the SIF variability for the circumferentially oriented, axially loaded flaw because the flaw is located on the shell-side of the weld where the interlayer gaps run into the weld and the gaps result in localized bending stress. Note that the relative influence of the weld material properties on weld residual stress variation is dependent on the location of the flaw in the H-S weld. As expected, the shell material properties are relatively more significant for the circumferentially oriented, axially loaded flaw, whereas the head material properties are relatively more significant for the axially oriented, hoop loaded flaw, which is located on the head-side of the weld. Interactions between the random variables were negligible in this analysis. Ultimately, this result indicates that thickness and weld width variation have a minimal contribution to the overall SIF variability for the two reference flaw locations and geometries evaluated in this study.

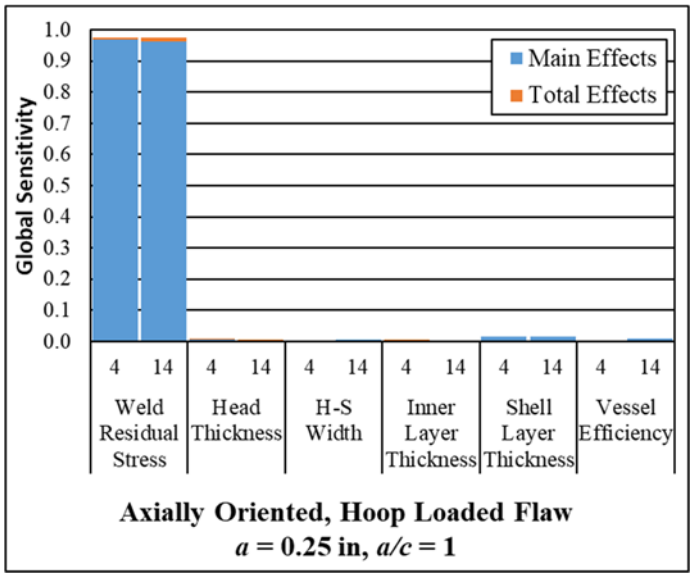

FIGURE 12: GLOBAL SENSITIVITY ANALYSIS OF THE SIF FOR THE AXIALLY ORIENTED, HOOP LOADED FLAW WITH FLAW GEOMETRY a = 0.25 *in* AND a/c = 1. THE SENSITIVITY RESULTS WERE NEARLY IDENTICAL FOR FLAW GEOMETRY a = 0.2 *in* AND a/c = 2/3.

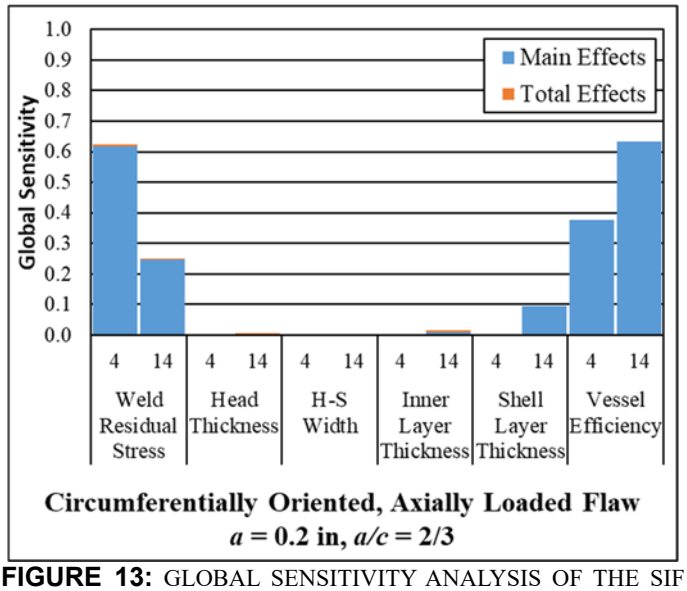

FIGURE 13: GLOBAL SENSITIVITY ANALYSIS OF THE SIF FOR THE CIRCUMFERENTIALLY ORIENTED, AXIALLY LOADED FLAW WITH FLAW GEOMETRY a = 0.2 *in* AND a/c = 2/3. THE SENSITIVITY RESULTS WERE NEARLY IDENTICAL FOR FLAW GEOMETRY a = 0.25 *in* AND a/c = 1.

NESSUS was used to generate the CDF for the SIF for each reference flaw in the 4- and 14-layer vessels. The CDF was converted to a PDF and compared to a preliminary value of the upper shelf of the elastic-plastic fracture toughness measured in a weld heat-affected zone (K_{JC}: Normal with μ=68, σ=6.8 ksi$\sqrt{\text{in}}$). A COV of 10% was estimated for the fracture toughness distribution based on expert opinion from the metallics community. These PDFs are shown in Figure 14 for the 4-layer vessel and Figure 15 for the 14-layer vessel. There was overlap between the SIF and toughness PDFs for the 4-layer vessel, resulting in an estimated probability of the K_I exceeding K_{JC} of 0.027 and 0.0002 for the "a" and "c" tip respectively, using Eq. (2) and (3) and Monte Carlo sampling to perform the integration.

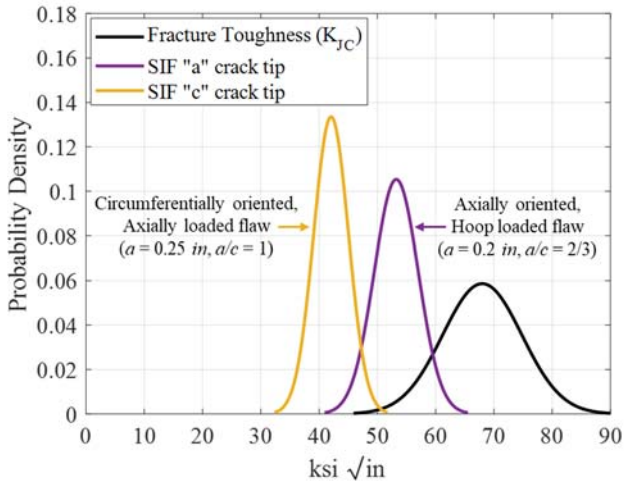

FIGURE 14: STRESS INTENSITY COMPARED TO THE ELASTIC-PLASTIC FRACTURE TOUGHNESS FOR THE 4-LAYER VESSEL AT THE TWO REFERENCE FLAW LOCATIONS

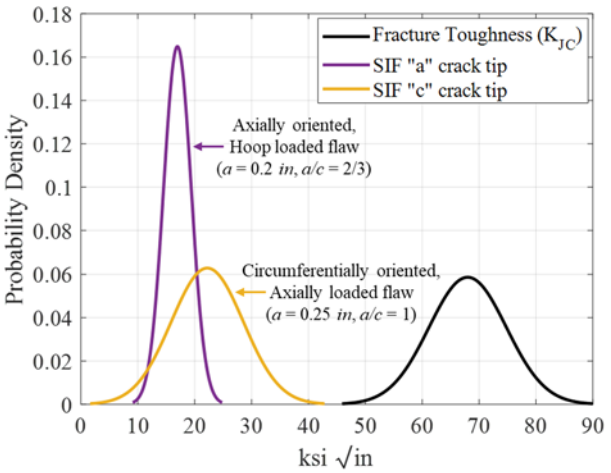

FIGURE 15: STRESS INTENSITY COMPARED TO THE ELASTIC-PLASTIC FRACTURE TOUGHNESS FOR THE 14-LAYER VESSEL AT THE TWO REFERENCE FLAW LOCATIONS

The 14-layer vessel probability of failure is essentially zero because of the large separation of the SIF and toughness PDFs. These predictions are largely driven by uncertainties in the WRS models/data and assumption of the fracture toughness variation.

CONCLUSIONS

A probabilistic framework was developed to predict the structural integrity of a fleet of LPVs. Probabilistic studies were performed to predict the variability in the SIF and probabilistic sensitivity studies were performed to identify the model parameters influencing this variability. The results of this study are preliminary in nature and are used primarily to demonstrate the framework and guide resource allocation for further development. Based on the results of this study, the WRS uncertainty is the largest driver of uncertainty in predicting the SIF. There is also considerable variation and uncertainty in the fracture toughness. Further efforts are underway to reduce uncertainties in the model predictions to reduce conservatism in the evaluation of these vessels.

This evolving framework includes models for WRS and operating stress gradients, SIF calculations using NASGRO, and fracture toughness. The V&V model development framework provides a systematic approach to identify and reduce uncertainties in the inputs and models and provide evidence of the predictive capabilities of the models. This framework can also utilize the fatigue crack growth and failure assessment diagram capabilities in the NASGRO software along with the stress gradient and fracture toughness models. Further development and evaluation of these tools are underway as one part of NASA's strategy to evaluate the safety of the LPV fleet.

ACKNOWLEDGEMENTS

This work was conducted under funding from the NASA Headquarters Office of Safety and Mission Assurance (OSMA).

REFERENCES

[1] Prosser, W. H., "Evaluation of Agency Non-code Layered Pressure Vessels (LPV's)", NASA/TM – 2014-218505/Volume I, NESC-RP-13-00852, Langley Research Center, July 2014.

[2] American Society of Mechanical Engineers. V&V 10 – 2006. "Guide for verification and validation in computational solid mechanics, American Society of Mechanical Engineers", C06906, New York, NY, 2006.

[3] Cowles, B., Backman, D., and Dutton, R., "Verification and validation of ICME methods and models for aerospace applications", Integrating Materials and Manufacturing Innovation, 1(1), p. 2, 2012.

[4] Saltelli, A., Annoni, P., Azzini, I., Campolongo, F., Ratto, M., and Tarantola, S., "Variance based sensitivity analysis of model output. Design and estimator for the total sensitivity index", Computer Physics Communications, 181(2), pp. 259-270, 2010.

[5] McFarland J. M., Riha D. S., "Probabilistic Analysis using NESSUS (Numerical Evaluation of Stochastic Structures Under Stress)", Handbook of Uncertainty Quantification, R. Ghanem, D. Higdon, and H. Owhadi, eds., Springer International Publishing, Cham, pp. 1733-1764, 2017.

[6] American Society of Mechanical Engineers. 2017. Boiler and Pressure Vessel Code, Section VIII, Division 1. New York: ASME.

[7] Hobbs, J. R., "Calculation of Stress Intensity Factors for Layered Pressure Vessel Inner Layer Through Cracks", Proceedings of the 2019 ASME PVP Conference, San Antonio, TX.

[8] Jawad, M. H., "Theory and Design of Plate and Shell Structures", Chapman & Hall, Inc., 1994.

[9] User Manual for VFT – Virtual Fabrication and Weld Modeling Software by Engineering Mechanics Corporation of Columbus (EMC^2), Battelle Memorial Institute and Caterpillar Inc., April 2016.

[10] Brust, F. W., Dodds R. H., Hobbs, J. R., Stoltz, B., and Wells, D., "Weld Residual Stress and Fracture Behavior of NASA Layered Pressure Vessels", Proceedings of the 2019 ASME PVP Conference, San Antonio, TX.

[11] NASGRO® Fracture Mechanics and Fatigue Crack Growth Analysis Software, Version 9.0, NASA Johnson Space Center and Southwest Research Institute, May 2018.

[12] Rasmussen, C. E. and Williams, K. I., "Gaussian Processes for Machine Learning", MIT Press, 2006.

[13] Higdon, D., Gattiker, J., Williams, B., and Rightley, M., "Computer model calibration using high-dimensional output", Journal of the American Statistical Association, Vol. 103, No. 482, pp. 570-583, 2008.